Journal of Hydrology (NZ) 61 (2): 113-136

The hydroelectric power potential of New Zealand's largest catchment (Clutha River) under 21st century climate change

Andreas M. Jobst, Nicolas J. Cullen* and Daniel G. Kingston
School of Geography, University of Otago, Dunedin, New Zealand
**Corresponding author: nicolas.cullen@otago.ac.nz*

Abstract

With major alterations in the regimes of snow-fed mid-latitude rivers projected for the end of this century, the output from hydroelectric river run-off schemes will potentially be affected to a similar extent. While resulting changes in the annual and seasonal power output have been investigated for a number of catchments, more transparency is needed in terms of dominant mechanisms driving these changes and model component-specific uncertainty. In this study an ensemble of 32 hydrological simulations is used to investigate the hydroelectric power potential of the Clutha River (Southern Alps, New Zealand) under 21st century climate change. The ensemble encompasses two emission scenarios, four General Circulation Models, two bias correction methods and two snow models. The fully distributed hydrological model WaSiM is used to model both the main natural processes and major forms of water management in the catchment. The catchment's largest hydroelectric scheme is modelled by an external component. In the 2090s the results show substantial increases in the output for winter (18%) and spring (7%), followed by reductions in summer (-19%) and autumn (-4%). A net increase in annual streamflow does not lead to a corresponding increase in annual output, which is attributed to excess water being spilled during high flow events. The driving controls behind this are identified as more winter precipitation, a reduction in the solid fraction of precipitation and an increase in extreme precipitation events. The relatively large variation in the projected seasonal output is found to be primarily caused by the General Circulation Model and the emission scenario, while bias correction and the snow model made a smaller contribution to the overall uncertainty.

Keywords

hydroelectric power, climate change, uncertainty, New Zealand, hydrological model, snow model, snowmelt, extremes, low flow, high flow, spill

Introduction

Alpine catchments typically have a large potential for hydroelectric energy generation due to high annual precipitation totals. Natural stores, in particular seasonal snow and glaciers, play an important role as they accumulate potential energy (Arheimer *et al.*, 2017). Most of the stored energy then gets released during the main melt period. A change in the seasonality of precipitation has a direct impact on the seasonal streamflow regime (Jobst *et al.*, 2018b), which then affects the energy output of hydroelectric schemes located downstream. Temperature is another important driver as it controls both snow accumulation and melt processes

(Cullen and Conway, 2015; Cullen *et al.*, 2019). As climate change will significantly alter both temperature and precipitation over the course of the 21st century (Collins *et al.*, 2013), the impacts on montane catchments can be expected to be considerable. Accordingly, many montane catchments are predicted to experience substantial shifts in their regimes and also changes in the magnitude of streamflow (Leung *et al.*, 2004; Kingston *et al.*, 2011; Shrestha *et al.*, 2012).

Regarding the implications of climate change for hydroelectric schemes, projected changes in the annual output have generally been found to be small with variable directions of change (Koch *et al.*, 2011; Majone *et al.*, 2016; Wagner *et al.*, 2017). As such, depending on the selected General Circulation Model (GCM), at the end of the 21st century the change in hydroelectric power potential of the Pacific Northwest (USA) is projected to range from positive to negative values (i.e., -25 to 10%) (Markoff and Cullen, 2008). Larger projected annual changes with a uniform direction of change (15–30% and above for the 2070s) were reported by Lehner *et al.* (2005) for Scandinavia, northern Russia and Iceland, which they attributed to changes in the precipitation patterns. The study of Minville *et al.* (2008) found that, despite an increase in annual inflows, annual output is projected to decrease. The driving mechanism was identified to be an earlier spring flood, which under the current water management would result in an increase in unproductive spills.

Seasonal hydroelectric power output from alpine rivers is thus projected to undergo larger changes. The main mechanism described is a shift in the timing of the peak melt volume altering the monthly regime of rivers, which directly impacts hydroelectric power output (Beniston and Stoffel, 2014). Accordingly, an increase in output during winter and spring accompanied by a decrease in summer is projected for the European Alps (Koch *et al.*, 2011; Majone *et al.*, 2016; Wagner *et al.*, 2017), the Pacific Northwest (Hamlet *et al.*, 2010), South America (Popescu *et al.*, 2014) and the Southern Alps of New Zealand (Caruso *et al.*, 2016). These seasonal changes can cause challenges for water management and potentially a conflict of interest between different water users, especially if seasonal reductions in flow coincide with peak demand for irrigation and hydroelectric power (Singh and Bengtsson, 2004). The flattening of the flow regime has been reported to reduce the need for artificial water storage (Golombek *et al.*, 2012), as substantial amounts of the peak melt volume are shifted from spring to winter. However, a reduced temporal buffer of the snowpack could result in more spills, which would require an increase in storage capacity (Madani and Lund, 2010).

Studies of climate change impacts on hydroelectric power are subject to similar uncertainties as those focussed only on changes in hydrological variables. Liu *et al.* (2016) pointed out the importance of multi-model studies, as both the choice of the hydrological model and GCM caused a large range in their hydroelectric power projections for China. In Quebec, the combined uncertainty of GCM and emission scenario has been reported to vary seasonally, becoming largest during the spring flood period (Haguma *et al.*, 2014). In addition to the climate model, the parameterisation of the hydrological model also substantially affected the water availability of a hydroelectric power scheme in a glacierised catchment (Finger *et al.*, 2012).

In New Zealand, 60% of the national electricity supply is generated from hydroelectric power schemes (Ministry of Economic Development, 2012). This corresponds to a capacity of 5252 MW (Ministry of Economic Development, 2012) of which 65% is generated by hydroelectric plants located in the South Island. Despite New Zealand's strong dependence on

hydroelectricity, climate change impacts on hydroelectricity have only been investigated quantitatively for the Upper Waitaki catchment (Caruso *et al.*, 2016). Using averaged precipitation and temperature projections based on an ensemble of 12 GCMs and one emission scenario as input for a hydrological model, electricity generation was projected to increase for winter and spring with a decrease for summer (albeit less pronounced) (Caruso *et al.*, 2016). Other studies in New Zealand focusing on changes in natural flow have assumed that a flattening of the monthly regime could result in less water having to be redistributed via reservoirs, thus reducing the need for artificial storage (Poyck *et al.*, 2011; Gawith *et al.*, 2012; Hendrikx *et al.*, 2012).

As indicated by Jobst *et al.* (2018b) the spread in the seasonal streamflow signal can be large for climate change projections in the Southern Alps, with various model components contributing to the overall uncertainty (i.e., GCM 44–57%, emission scenario 16–49%, bias correction 4–22% and snow model 3–10%). Thus, the uncertainties in hydroelectric projections also need to be assessed (as suggested by Caruso *et al.*, 2017) as they could be of a similar or even greater magnitude as changes in streamflow.

This study focuses on New Zealand's largest catchment, the Clutha River, with the purpose to assess the hydroelectric power potential of its main scheme (Clyde: ~13% of the South Island's capacity) under 21st century climate change. The Clutha integrates all of the main characteristics of an alpine snow-fed, mid-latitude catchment and the findings from this study are expected to be of interest to future studies focusing on catchments with a comparable hydroclimate.

The fully distributed hydrological model WaSiM (Schulla, 2012), as described in Jobst *et al.* (2018b), was implemented to generate daily simulations of streamflow, which were then used to calculate seasonal and annual hydroelectric power generation. Uncertainties in the projections were investigated using an ensemble of four GCMs, two emission scenarios and two bias correction methods. WaSiM was run with two different snow models in order to also include the uncertainty linked to snowmelt, which is a key process in the upper Clutha catchment.

The primary aim of this paper is to quantify the potential annual and seasonal changes in hydroelectric power output for the Clutha catchment. In addition to investigating the seasonal hydropower signal and identifying the dominant uncertainty sources, this study will also identify the driving physical processes behind changes in power output by investigating flow extremes, the role of the snow storage and changes in extreme precipitation.

Data and methods

The study domain

The Clutha catchment is the largest catchment in New Zealand by area (20,586 km^2) and has the highest mean flow (570 $m^3 s^{-1}$). The Clutha's headwaters are located on the eastern side of the Southern Alps (lower South Island), and the catchment extends to the east coast of the South Island (Fig. 1). The Clyde Dam (and associated hydroelectric power station) is located in the central part of the basin with a catchment area of 12,212 km^2 and a mean flow of 491 $m^3 s^{-1}$. The climate of the catchment is under the predominant influence of the westerly wind belt. Average annual precipitation totals exceed 12,000 mm along the main divide and decrease sharply towards the centre of the catchment (~500 mm). The annual contribution of snowmelt to runoff varies across the catchment and was estimated by Kerr (2013) to range from 11 to 13% for inflows to the three headwater lakes Wakatipu, Wanaka and Hawea. Jobst *et al.*

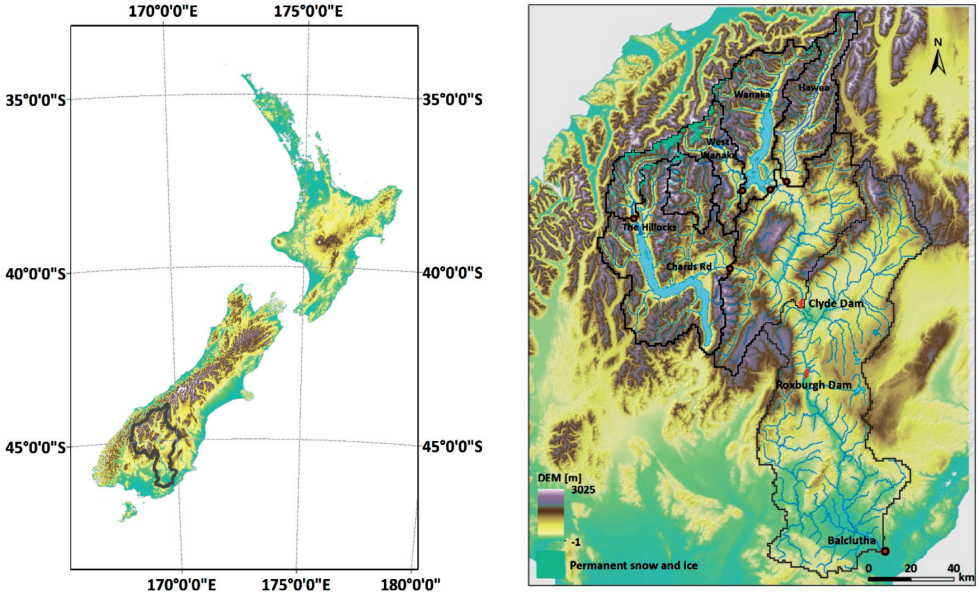

Figure 1 –The location of the Clutha catchment in New Zealand (left) and the catchment of the hydroelectric scheme at Clyde (right). Subcatchments of relevance to this study and other main sites are also shown.

(2018b) found the proportion of snowmelt to be higher (i.e., 16–21%), which can be expected to be substantially higher during winter and spring. The ice-covered area in the catchment is relatively small and was estimated by Chinn (2001) to be 147 km^2, which corresponds to 1.2% of the catchment area above the Clyde Dam.

Two large hydroelectric power plants are located in the central part of the catchment and together account for approximately 22% of the South Island's total hydroelectric power capacity. The plant in Clyde has a greater capacity (432 MW) than the Roxburgh scheme located ~33 km downstream (320 MW). The operator, Contact Energy, controls the outflow of Lake Hawea, while the outflows at lakes Wakatipu and Wanaka are natural and not managed. The operational volume for Hawea of 2.3 km^3 can sustain the mean flow at Clyde for ~54 days. Projections for Roxburgh were found to be very similar due to the relatively small additional flow received from the Manuherikia catchment (occupying most of the area between Clyde and Roxburgh), and therefore the results in this paper are only shown for the scheme at Clyde.

The WaSiM model of the Clutha

The physically oriented and fully distributed hydrological model WaSiM was implemented for the Clutha catchment following Jobst *et al.* (2018b). Input variables to WaSiM comprised spatially interpolated station-based data for air temperature, precipitation, solar radiation, relative humidity and windspeed, interpolated as described in Jobst *et al.* (2017, 2018a). Importantly, temperature and precipitation fields were not based on the commonly used Virtual Climate Station Network (Tait *et al.*, 2006), but rather a modified approach that resulted in improved root mean square error and bias statistics (Jobst *et al.*, 2017, 2018a). In addition to the key natural processes (unsaturated zone and

groundwater flow, snow accumulation and melt, glacier dynamics, evapotranspiration), the major forms of water management (i.e., weir at Lake Hawea and irrigation takes) were also modelled. WaSiM's lake model was set up for the two natural lakes (Wakatipu and Wanaka) and the management model for the dam at Lake Hawea. The management of the weir is complex, as it depends on electricity price, inflows and seasonal climate outlooks. Considering the complexity of the management system and the monthly to seasonal focus of this study, only the main operating rules were implemented, with the emphasis on a realistic simulation of the historic (1992–2012) outflow regime:

- Maximum operational flow 200 $m^3 s^{-1}$ (1 February to 31 August)
- Maximum operational flow 60 $m^3 s^{-1}$ (1 September to 31 January)
- Minimum operational flow 10 $m^3 s^{-1}$ (1 September to 31 January)

Irrigation takes in the Clutha catchment are substantial and amount to approximately 73 $m^3 s^{-1}$ (Otago Regional Council, 2008), which corresponds to ~13% of the Clutha's average flow. In Otago, the irrigation season runs from October to April and most schemes have an approximate efficiency (proportion of abstracted water effectively absorbed by plants) of 60% (Kienzle and Schmidt, 2008). Irrigation takes were modelled conceptually by abstracting water from the outlets of subcatchments (with an effective water loss of 60%) based on information from Otago Regional Council (2008). To allow for the snow model-related uncertainty analysis, two implementations of WaSiM were set up, with the snow melt routine solved by a simple temperature index (Tindex) approach and the conceptual energy balance model of Anderson (1973), respectively (described in Schulla, 2012).

WaSiM was calibrated for the four-year period between 2008 and 2012 and subsequently validated over the longer 1992–2008 period, as described in more detail by Jobst *et al.* (2018b). Calibration was an iterative process, based on a combination of manual parameter optimisation followed by autocalibration using the Particle Swarm technique (Jiang *et al.*, 2010). To quantify the performance of the model, three performance criteria were used by Jobst *et al.* (2018b), based on Equation 1: the Nash-Sutcliffe model coefficient of efficiency (NSE) based on daily data, log-transformed daily data (NSE_{log}) and monthly data (NSE_{mo}). NSE_{log} was calculated in addition to the standard NSE and NSE_{mo} in order to reduce the emphasis of the performance indicator on flood peaks. The Nash-Sutcliffe model coefficient of efficiency (NSE) is defined as:

$$NSE = 1 - \frac{\sum_{i=1}^{n}(O_i - M_i)^2}{\sum_{i=1}^{n}(O_i - \bar{O})^2} \quad (1)$$

The evaluation of WaSiM revealed a strong model performance at the outflows of the two natural lakes, albeit with some overestimation of monthly flow during the autumn months of April and May and underestimation of the highest daily flows (Fig. 2). The two WaSiM model versions (one based on the Anderson (1973) approach and one based on the Tindex snowmelt routine) perform similarly for Lake Wanaka outflows. For the Chards Road site (catchments of Lake Wakatipu and Shotover River; see Fig. 1), the Anderson method results in underestimation of river flow during July and August, while the Tindex version underestimates flows in November and December. As reported by Jobst et al. (2018b), daily and monthly NSE values indicate excellent model performance, ranging between 0.86 and 0.90 (Table 1). In recognition that the strong seasonality of Clutha river flows may lead to the generation of high NSE values irrespective of model performance, an additional step was taken to calculate the NSE for daily data on a monthly basis (i.e., NSE across all January days, all

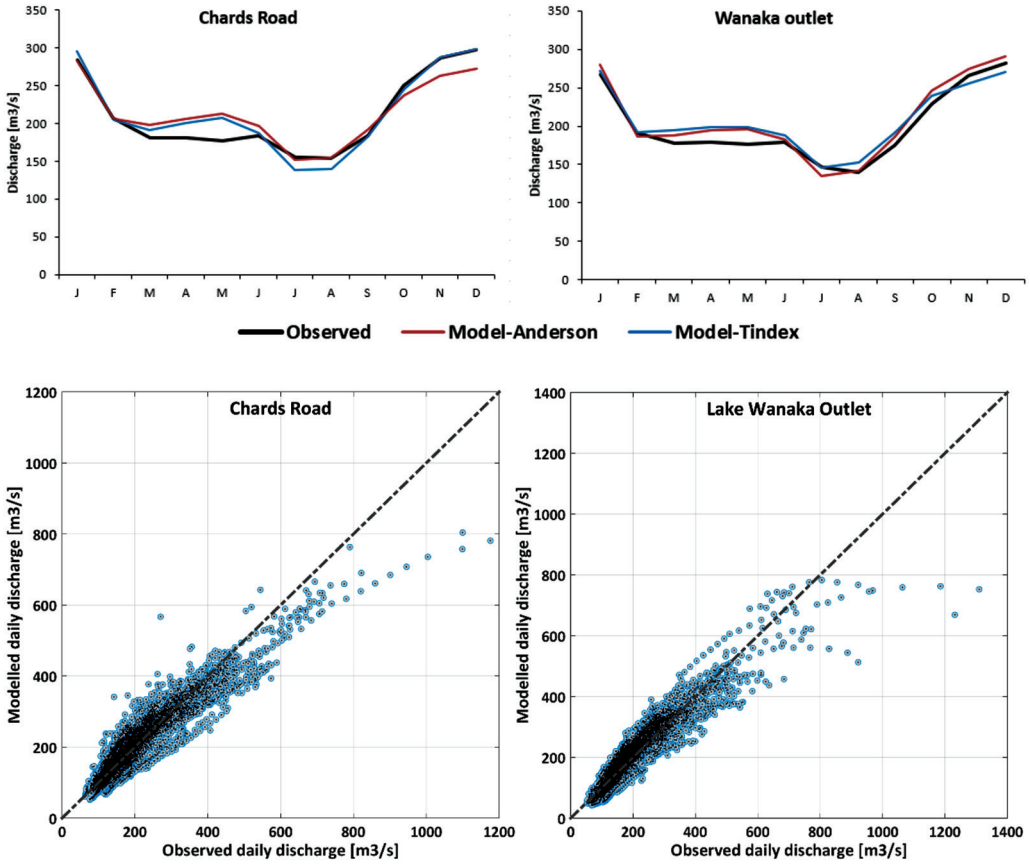

Figure 2 – Chards Road and Wanaka outlet mean monthly observed and modelled river flow (Anderson and Tindex) (upper plots), and relationship between observed and modelled (Anderson) daily mean flow (lower plots).

Table 1 – Performance criteria for modelled streamflow at various gauges in the Clutha catchment for WaSiM-Anderson (WaSiM-Tindex) as computed for the validation period (1992–2008).

Gauge	NSE	NSElog	NSEmo
Chards Rd	0.87 (0.85)	0.86 (0.86)	0.89 (0.87)
Lake Wanaka outlet	0.87 (0.87)	0.87 (0.88)	0.90 (0.90)
Lake Hawea outlet	0.22 (0.21)	0.25 (0.25)	0.41 (0.40)
The Hillocks	0.64 (0.65)	0.64 (0.68)	0.78 (0.79)
West Wanaka	0.62 (0.62)	0.72 (0.72)	0.83 (0.82)
Clyde	0.78 (0.78)	0.73 (0.74)	0.85 (0.84)

February days, etc.) for Chards Road and Wanaka outflows (Table 2). Although lower NSE values occur in May, July and August for Chards Road in particular (0.68 for the Tindex model at Chards Road in May is the lowest), these still indicate generally strong model performance and are comparable with previous studies of the Clutha (Poyck et al. 2011; Gawith et al., 2012) and Waitaki (Caruso et al., 2017).

Table 2 – Monthly separation of daily NSE values for WaSiM Anderson (Tindex) at Chards Rd and Lake Wanaka outlet.

Month	Chards Rd	Lake Wanaka outlet
January	0.88 (0.89)	0.85 (0.86)
February	0.86 (0.86)	0.86 (0.84)
March	0.87 (0.84)	0.86 (0.83)
April	0.85 (0.82)	0.84 (0.82)
May	0.72 (0.68)	0.84 (0.81)
June	0.81 (0.80)	0.87 (0.87)
July	0.63 (0.74)	0.79 (0.83)
August	0.70 (0.78)	0.81 (0.77)
September	0.78 (0.78)	0.81 (0.77)
October	0.84 (0.83)	0.85 (0.86)
November	0.84 (0.81)	0.81 (0.82)
December	0.87 (0.81)	0.90 (0.90)

The validation results for the two headwater gauges West Wanaka and the Hillocks are also displayed to show the performance of the model without any potential smoothing effect of the lakes on the daily discharges. The NSE values range between 0.62 and 0.82 for the three indicators at the two gauges, still reflecting a good model performance albeit lower than the NSE values for the lake outflows. At Lake Hawea, the low NSE values show that the variability of daily (NSE of 0.21) and monthly (NSE of 0.41) streamflow is not sufficiently captured by the management model, which was parameterised to reproduce the 20-year regime. It needs to be noted that, based on the mutual data period between Clyde and the lake outflow records (1997–2012), on average 42% of the discharge at Clyde stems from the Kawarau subcatchment (see gauge Chards Rd in Fig. 1) and 40% from outflow at Lake Wanaka. The contribution of the Hawea outflow (i.e., 12%) is comparatively small, which explains the only moderate downstream effect of the poor model performance at Hawea on the modelled streamflow at Clyde (NSE values from 0.73 to 0.85).

Regarding the role of the snowpack, the relative proportions of the total snow water equivalent (SWE) volume during winter were modelled as follows for different elevation bands: 3% (≤ 1000 m), 35% (1001–1500 m), 54% (1501–2000 m) and 8% (> 2000 m). Hence, the relative change of SWE between 1001 and 2000 m will affect the total SWE volume more strongly than changes in the remaining two bands. While changes above 2000 m could still have a significant impact, changes in the lowest band are clearly the least important.

The hydropower model

The hydroelectric power was calculated as a function of kinetic and potential energy, with the two main parameters being hydraulic head and streamflow. The hydroelectric power generation at Clyde was then calculated using Equations 2 and 3:

$$Pc = \eta e \cdot \rho \cdot Q \cdot g \cdot H \quad (2)$$

where Pc is the capacity (kW) for a certain time period, ηe is the efficiency factor of the hydroelectric power plant, ρ is the density of water (1000 kg m^{-3}), Q is the streamflow (m^{3}s-1), g is the gravitational acceleration (9.81 m s^{-2}) and H is the hydraulic net head (m). The daily hydroelectric power generation (E) (kWh) can then be solved as:

$$E = Pc \cdot t \quad (3)$$

where t is time (24 h).

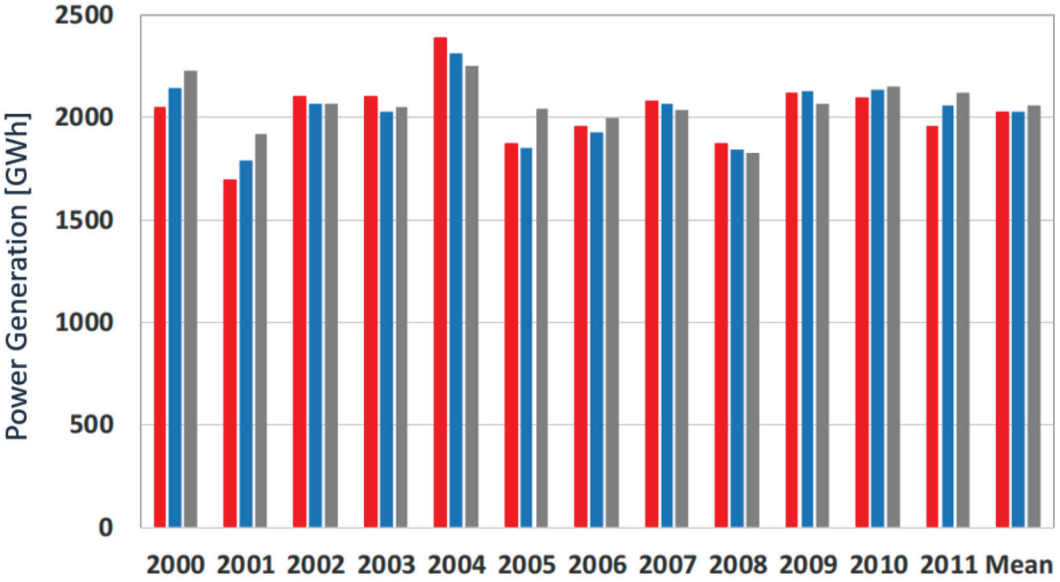

Figure 3 – The annual power generation at Clyde (GWh). The red bars represent the annual production as provided by Contact Energy. The production based on the hydroelectric power model forced by observed streamflow (Emod_Qobs) and modelled streamflow (Emod_Qmod) are shown in blue and grey, respectively.

The maximum operational flow of 950 $m^3 s^{-1}$ at Clyde is rarely met, primarily due to servicing and the prioritisation of other energy sources (i.e., wind) in the New Zealand electricity market. A manual approximation of the effective maximum operational flows with the objective to minimise the mean annual output error was performed, resulting in an effectively used maximum operational flow of 560 $m^3 s^{-1}$.

Figure 3 shows the simulated power generation (2000–11) compared to the official output using either observed streamflow (Emod_Qobs) or modelled streamflow (Emod_Qmod). For the mean annual output, Emod_Qobs has a minor positive bias at Clyde (0.1%). The mean annual bias of Emod_Qmod, which is directly linked to over- and underestimations of modelled streamflow, is slightly more pronounced but still acceptable at 1.8%. Monthly or seasonal output data were not available and therefore no seasonal validation could be carried out.

The climate model ensemble

Daily Regional Climate Model (RCM) simulations (provided by NIWA) forced by eight GCM simulations based on four CMIP3 GCMs (CM2.1-GFDL, ECHAM5, HadCM3 and MK3.5-CSIRO) and two emission scenarios (A1B and A2) were bias corrected and downscaled to the 1 km grid of the hydrological model. Two different bias correction methods, linear transformation (LT; as described in Lenderink *et al.*, 2007) and quantile mapping (QM; as described in Mpelasoka and Chiew, 2009), were run followed by a mass- and energy-conserving downscaling approach. The downscaling step was required to bridge the gap between the HadRM3P RCM (~27 km) and the hydrological model (1 km). The individual model components and processing steps are described in more detail in Jobst *et al.* (2018b). Forcing WaSiM-Anderson and WaSiM-Tindex with the 16 downscaled climate projections (2 emission scenarios, 4 GCMs

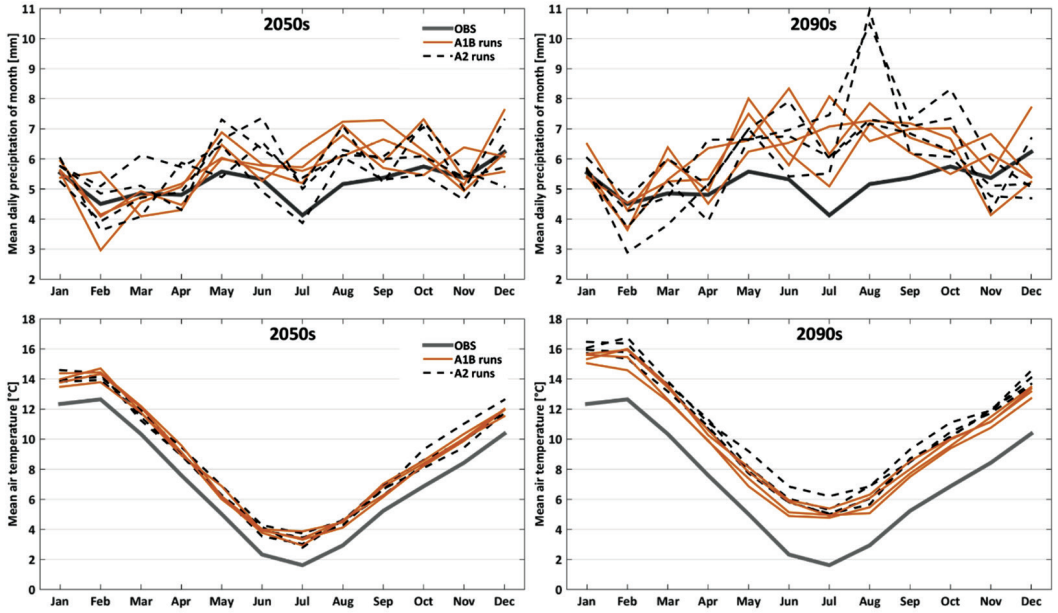

Figure 4 – The monthly climate regimes for the 2050s and 2090s periods for two variables: precipitation and mean air temperature. The baseline climate (1992–2011) is represented by the grey line.

and 2 bias correction methods) resulted in a total of 32 hydrological simulations.

Results

The temperature signal (Fig. 4) shows a uniform increase for the monthly regime for both time periods. The annual temperature signal under the A1B (A2) scenario equates to 1.51°C (1.55°C) and 2.80°C (3.49°C) for the 2050s and 2090s, respectively. Changes in monthly precipitation (Fig. 4) are more variable with more pronounced changes for the 2090s (e.g., August range: 28–112%). All simulations show an increase during winter and early spring, while most simulations indicate a reduction in summer precipitation.

The changes in monthly streamflow are shown in Figure 5 using only the eight QM-Anderson runs (for clarity). Modifications of the historic regime are clearly more pronounced for the 2090s, but for both future periods streamflow is projected to increase from June to October and decrease in summer (December to February).

After running the external hydroelectric power model for the 32 hydrological projections of daily streamflow, annual changes were found to be rather small (Table 3). Seasonal changes were found to be relatively large (Fig. 6; Table 4) and follow closely the signal in the streamflow regime (Fig. 5). Hydroelectric power output is projected to increase substantially during winter and spring with a stronger signal for the 2090s (Fig. 6; Table 4). For the 2090s summer, large negative changes were modelled with the median change of the QM-Anderson sub-ensemble corresponding to approximately -6% of the historic annual output. When comparing the individual sub-ensembles, it can be seen that the QM-Anderson simulations are associated with the strongest signal and LT-Tindex simulations are associated with the weakest signal.

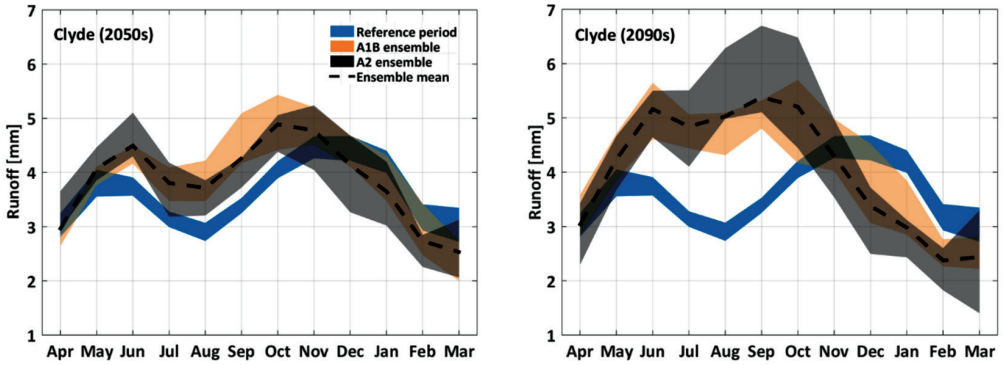

Figure 5 – Monthly runoff simulations for the 2050s and 2090s compared to the historic regime (only the QM-Anderson runs are shown).

Table 3 – Modelled relative change (%) for hydroelectric power and streamflow at the Clyde scheme.

	QM-Anderson	QM-Tindex	LT-Anderson	LT-Tindex	Mean
Hydropower					
2050s-A1B	1.8	1.6	1.5	1.2	1 .5
2050s-A2	0.0	-0.2	-0.3	-0.5	-0.2
2090s-A1B	3.7	3.0	3.0	2.5	3.0
2090s-A2	-1.8	-2.6	-1.6	-2.0	-2.0
Streamflow					
2050s-A1B	8.0	8.1	7.0	7.1	7.6
2050s-A2	5.7	5.9	4.9	5.0	5.4
2090s-A1B	13.4	13.5	11.4	11.5	12.5
2090s-A2	11.2	11.4	10.1	10.3	10.7

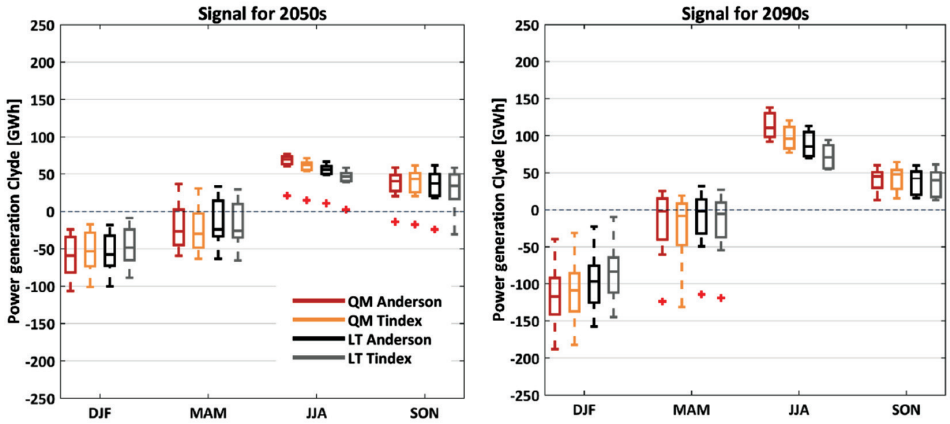

Figure 6 – Projected changes, relative to the refence period, in the seasonal hydroelectric power production (GWh) at Clyde for the 2050s (left) and 2090s (right). Each boxplot contains eight simulations based on the four GCMs and two emission scenarios.

Table 4 – Modelled relative seasonal change (%) for hydropower at the Clyde scheme.

	DJF	MAM	JJA	SON
2050s-A1B	-7.0	-5.0	11.1	6.6
2050s-A2	-13.2	-2.7	9.9	5.4
2050s-Mean	-10.1	-3.9	10.5	6.0
2090s-A1B	-14.3	0.8	18.5	7.4
2090s-A2	-23.9	-8.9	18.0	6.9
2090s-Mean	-19.1	-4.1	18.3	7.2

The mean decrease of -2% in output under the A2 emission scenario (and small increase of 3% under the A1B emission scenario) for the 2090s despite a relatively significant increase in annual streamflow (10.7 and 12.5% under A2 and A1B, respectively; Table 3) was found to be caused by a substantial increase in spills at the Clyde scheme. Spill amounts are substantial and were projected to range between 7 and 24% for the 2090s period with the potential for larger amounts under the A2 emission scenario (Fig. 7). Most of the additional spillover was projected to occur during winter and spring periods, when, in addition to higher monthly mean flows,

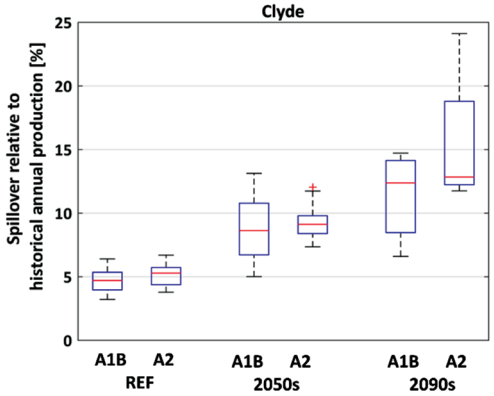

Figure 7 – The amount of mean annual spill for the three time periods and the two emission scenarios. Spill is depicted relative to the official historical (2000–11) annual production (i.e., 2027 GWh).

changes in the mean distribution of daily flows were also found. This is exemplified in Figure 8 for the ECHAM-A2 forced run, which shows a substantial increase of flow events exceeding the maximum capacity of the scheme (i.e., 700 $m^3 s^{-1}$), while events under the maximum capacity become less frequent.

Changes in the magnitude of extreme events were investigated using indicators of low flow (LF) and high flow (HF) events (Fig. 9) for a set of different return periods (2, 5, 10, 20, 50 and 100 years). The indicators were computed using a Pearson III distribution, with LF based on a 7-day duration. Although there is likely additional uncertainty associated with this particular choice of distribution and indicators, the relative direction of changes can be considered robust. As shown in Figure 9 (upper plot), high flow events are projected to increase in magnitude for all return periods except for HF-50y and HF-100y under the A1B emission scenario. The magnitude of high flow events is also substantially greater for the A2 simulations. The 7-day low flow event is projected to become increasingly extreme for higher return periods (Fig. 9, lower plot) with A2 simulations showing a consistently greater negative change in magnitude.

As indicated by Figure 9, both the A1B and A2 simulations contain a relatively large range for the low and high flow indicators (especially for higher return periods). The origin of the uncertainty that caused the large variation in the change of magnitude of the HF and LF indicators was further investigated and found to be composed of a number of model components. The approach of Muerth *et al.* (2012), which was used to assess the uncertainty signature of the seasonal streamflow signal for the north-western part of the Clutha catchment (Jobst *et al.*, 2018b), was used to identify the main uncertainty sources. The results are shown in Figure 10, where the bars represent the

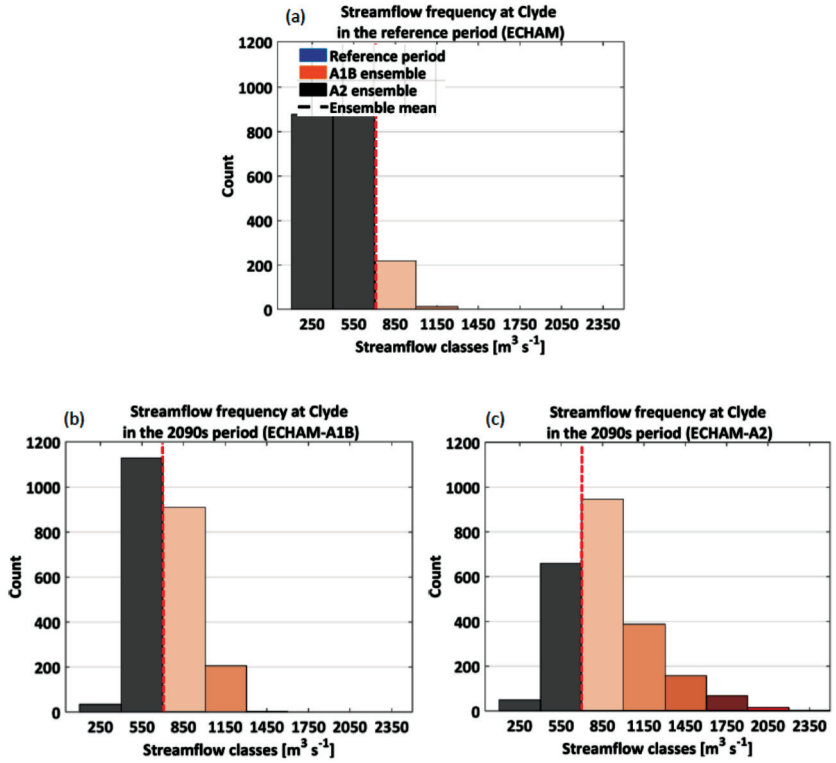

Figure 8 – The frequency distribution of daily streamflow between July and October at Clyde. The width of each class is 300 $m^3 s^{-1}$ with the mid-point labelled on the x-axis (e.g., the 550 $m^3 s^{-1}$ class ranges from 400 to 700 $m^3 s^{-1}$). The frequency distribution is shown for (a) the historic ECHAM5 run, (b) the 2090s ECHAM-A1B run and the (c) 2090s ECHAM-A2 run. The red line represents the (theoretical) maximum capacity of the scheme (700 $m^3 s^{-1}$).

relative contribution of a model component to the overall uncertainty and error bars represent the standard deviation (as explained in Muerth *et al.*, 2012, the standard deviation represents the dependence of an uncertainty source, e.g., GCM, on the other model components, e.g., emission scenario, bias correction and snow model). The results demonstrate that the GCM is the main source of uncertainty for both indicators (HF and LF) and all return periods. For the emission scenario, uncertainty becomes more important with higher return periods for the HF indicator and less important for LF. The emission scenario also has the largest standard deviation indicating a strong dependence on other model components (presumably the GCM). A moderate positive trend with return period can be seen for the bias correction method for both HF and LF. The contribution of the snow model to uncertainty is small for the HF indicators but more important for LFs, with its contribution exceeding the bias correction method for LF-2y and LF-5y.

The physical mechanisms driving the projected changes in streamflow frequency and extremes were also investigated, in particular the projected increase in flood events. One of the objectives was to determine if projected larger floods in the future (especially by the 2090s) are primarily

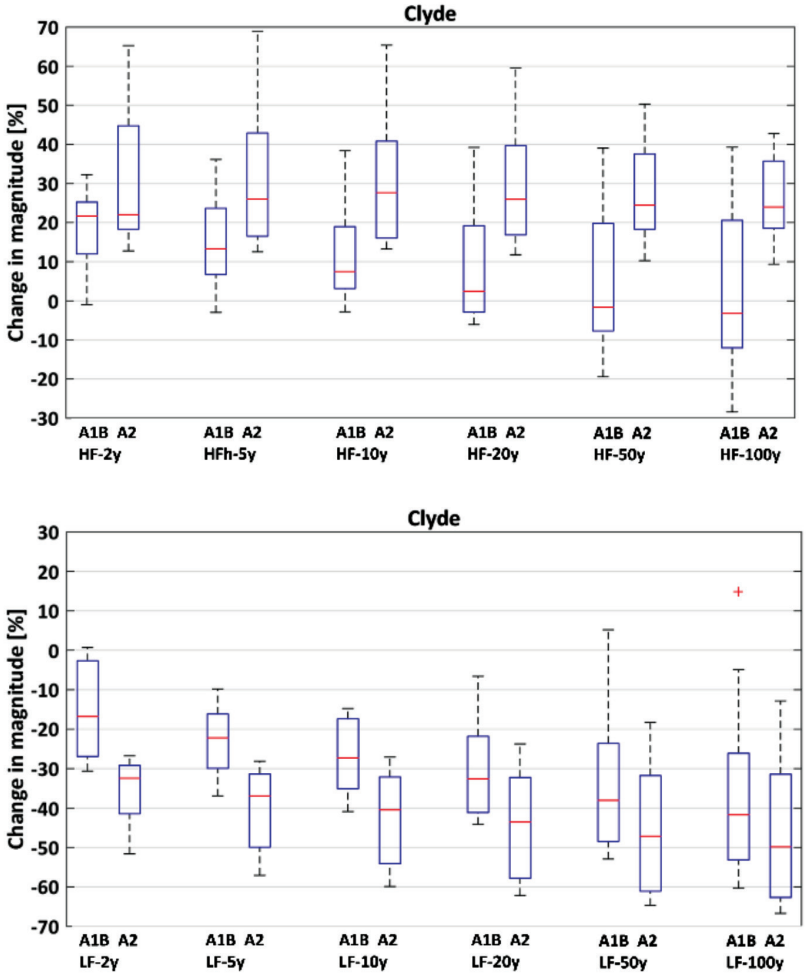

Figure 9 – Change (2090s) in the magnitude of high flow (top) and low flow (bottom) events for different return periods.

driven by an increase in winter precipitation (liquid fraction) or by a reduced snowpack. Regarding the latter, it was of interest to see if less snow accumulation due to higher temperatures (less snowfall) or changes in the melt regime (e.g., more melt events during winter) was the bigger contributor to the rise in flood events.

Figure 11 shows changes in the frequency of heavy precipitation events for the three headwater subcatchments Dart River, Matukituki River and Lake Hawea. (The corresponding gauges The Hillocks, West Wanaka and Hawea are shown on Fig. 1.) The three thresholds 90, 95 and 97.5 (corresponding to percentiles calculated during the reference period) were used and the relative change in the number of days exceeding each threshold is shown for the individual years from 1992 to 2099. While a positive trend can be seen for all subcatchments and thresholds, the trend is strongest for the Dart River.

With a moderate but significant increase in extreme precipitation events projected, changes in the solid fraction of these events

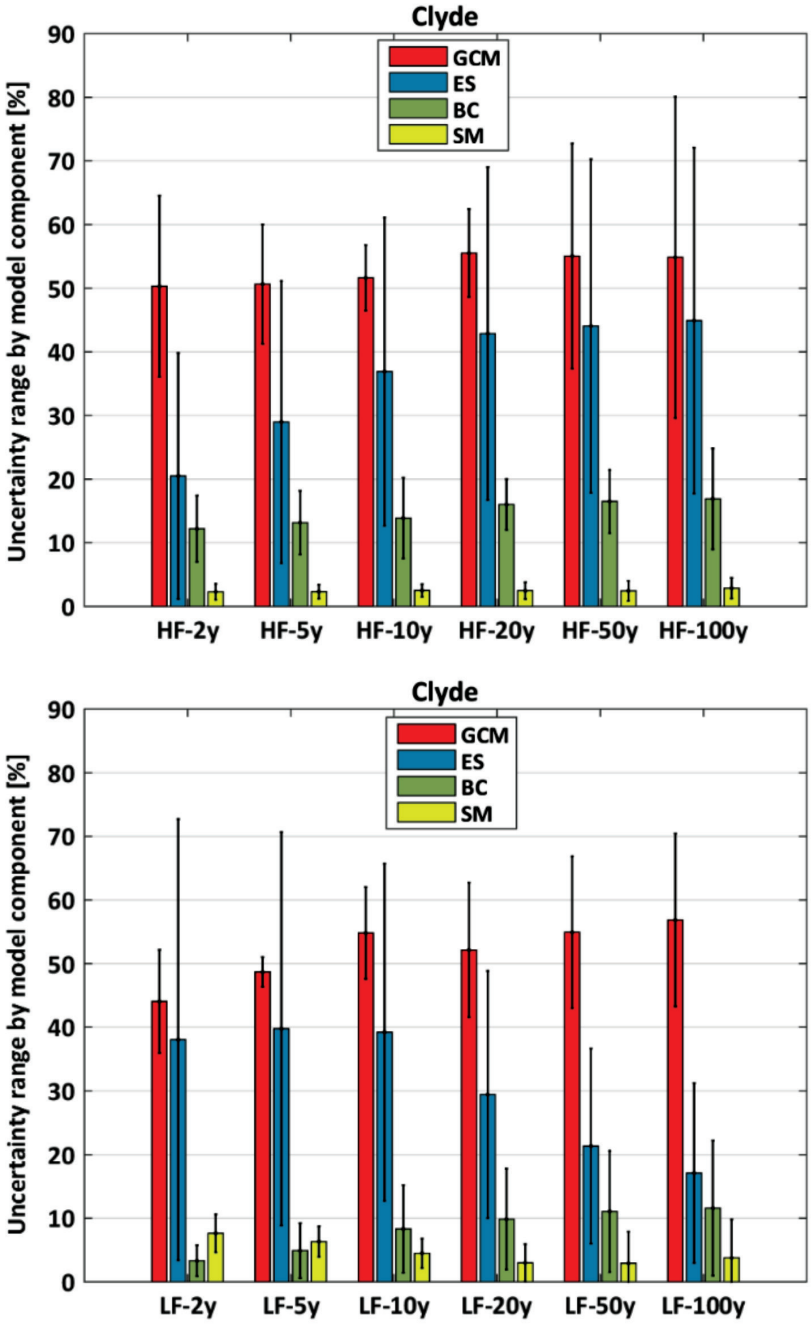

Figure 10 – The uncertainty range associated with the four model components General Circulation Model (GCM), emission scenario (ES), bias correction (BC) and snow model (SM) for different return periods of extreme flow events (2090s period only). The hydrological indicators are high flow events using the Pearson III distribution (top) and 7-day low flow using the Pearson III distribution (bottom). The uncertainty contributions were calculated as described in Jobst et al. (2018), adopted from Muerth *et al.* (2012).

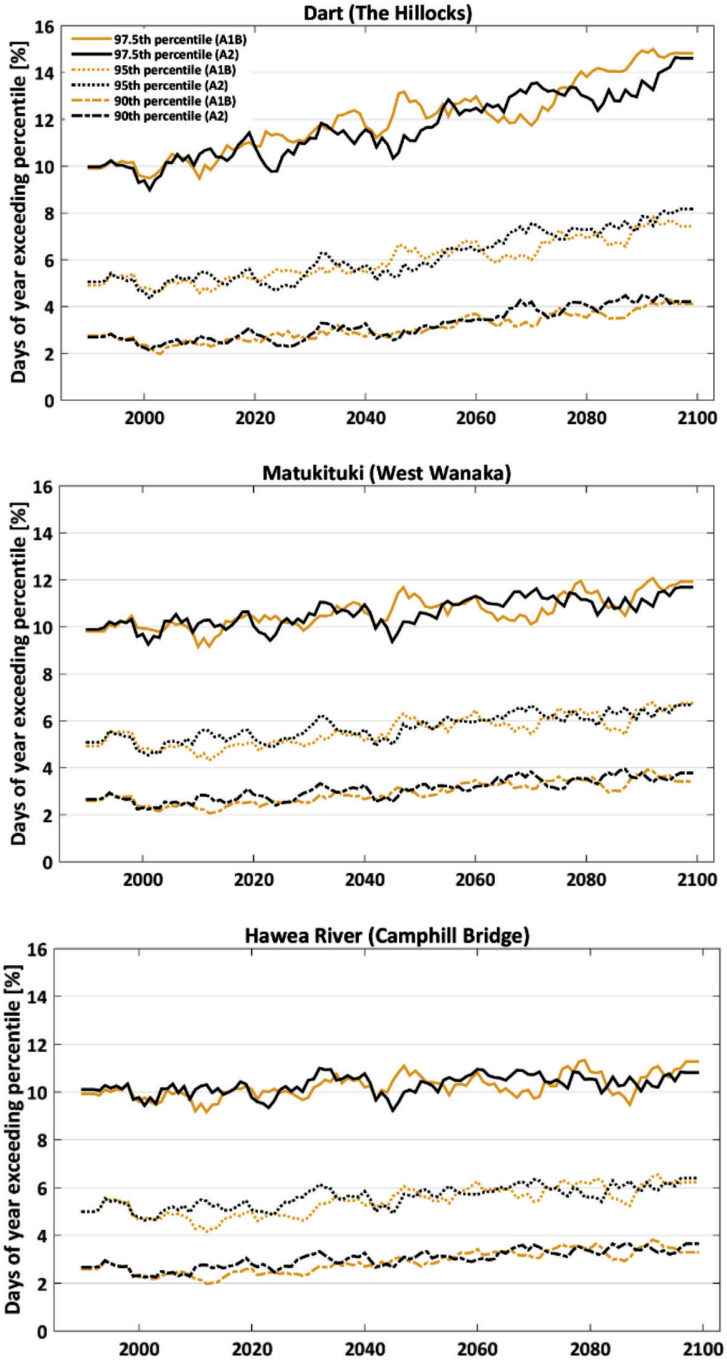

Figure 11 – Change in the frequency of heavy precipitation events for the north-west (top plot), the centre (middle plot) and the north-east of the headwaters (bottom plot) (see Fig. 1). Each plot shows the relative number of days above three different thresholds (i.e., percentiles) for the individual years (lines represent smoothed medians using a 5-day moving average). The three percentiles were calculated using the reference period (i.e., 1992–2011).

were investigated next. Heavy precipitation events (westerly storms) tend to bring substantial amounts of snow to the main divide and the headwaters of the Clutha, therefore having a strong control on the extent of the seasonal snowpack. Figure 12 shows changes in the solid fraction for these heavy precipitation events (only cells > 1000 m were included). For the Matukituki and Lake Hawea subcatchments, changes in the solid fraction are relatively consistent for the individual heavy precipitation thresholds. However, for the Dart subcatchment, the range is largest for the lower percentile (90th) and the median reduction in the solid fraction is weaker for the higher percentiles. Overall, a substantial reduction of the solid fraction is projected for all three classes of heavy precipitation events.

The annual (smoothed daily) regime of the proportion of melt (combined snow and ice) on total runoff (Qm_{prop}) is shown in Figure 13 for the WaSiM-Anderson and the WaSiM-Tindex simulations. The historical melt regimes are quite distinctive depending on which snowmelt routine is used. The

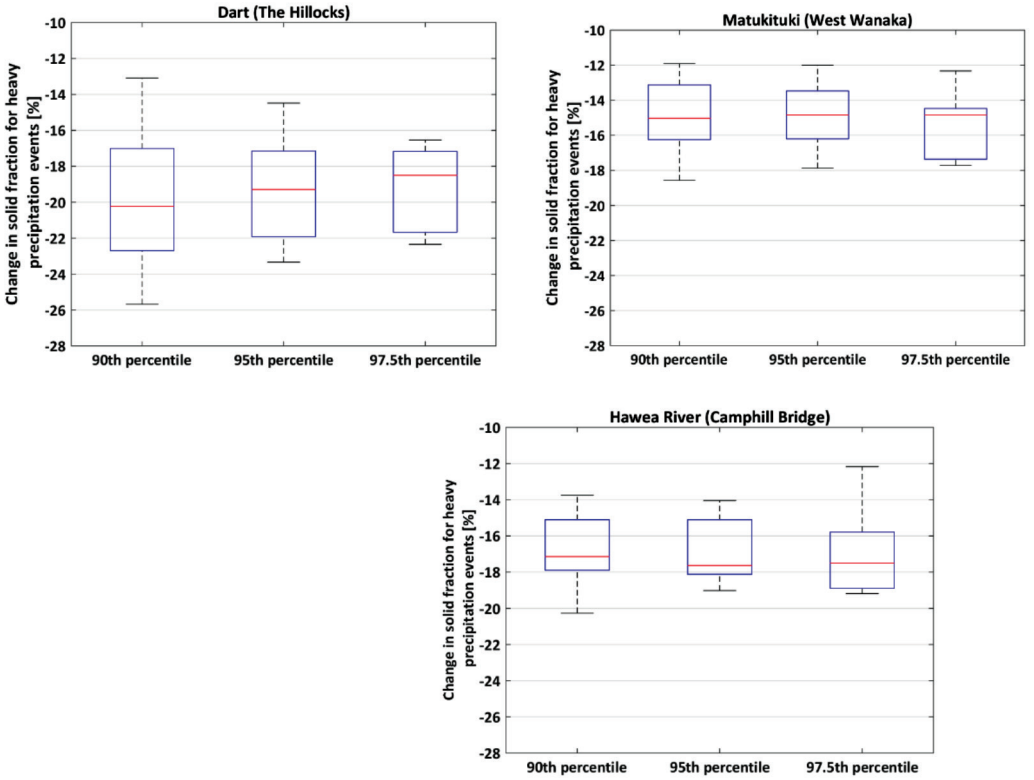

Figure 12 – The change (2090s vs. 2000s) in the solid fraction for heavy precipitation events exceeding various percentiles for the north-west (top left plot), the centre (top right plot) and the north-east (bottom plot) of the headwaters. The three percentiles stem from the distribution of the reference period and are calculated for each simulation separately. Each boxplot is based on 16 simulations (4 GCMs, 2 emission scenarios and 2 bias correction methods). The solid faction was calculated pixel-based for each precipitation event and then averaged for all cells >1000 m for the three subcatchments. The lower threshold of 1000 m was chosen because only 3% of the Clutha catchment's mean annual SWE volume was modelled below 1000 m.

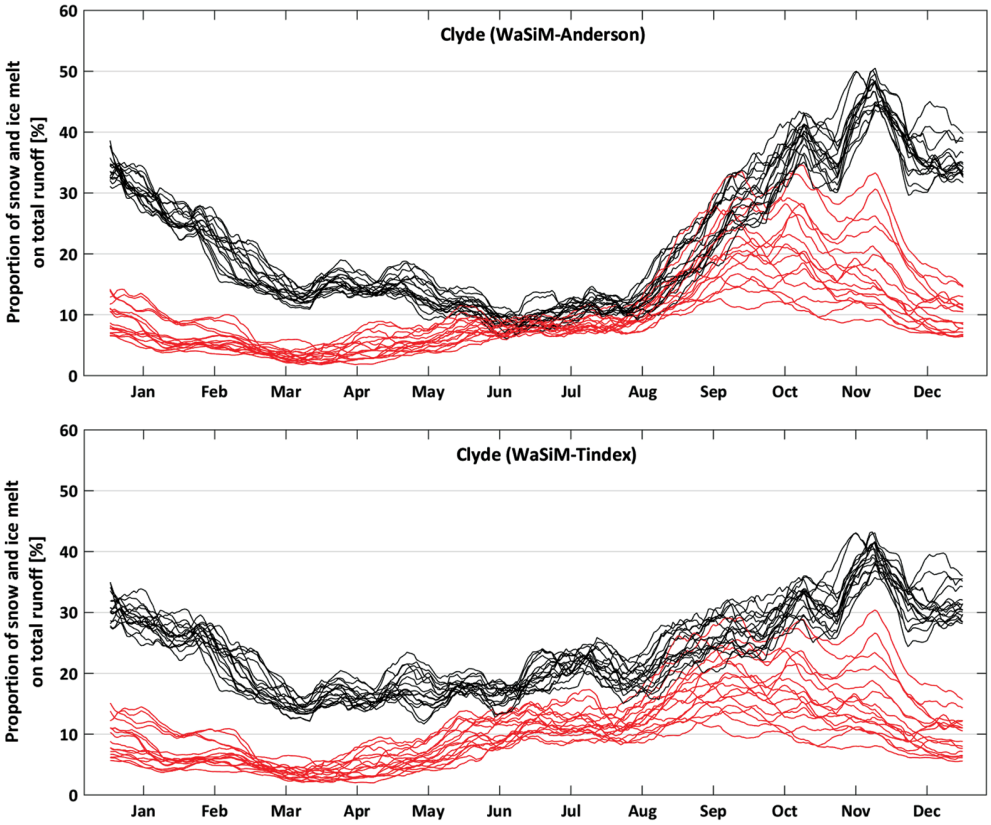

Figure 13 – Snow and ice melt as a proportion of total runoff averaged for the Clutha catchment (outlet Clyde) using WaSiM-Anderson (top) and WaSiM-Tindex (bottom). Historic simulations (black) are compared with the 2090s simulations (red). Daily simulations were first smoothed (14-day moving average) and then averaged for each Julian day of the corresponding time period.

main difference is the reduced seasonal amplitude for the Tindex simulations with a substantially smaller proportion during the seasonal melt peak in spring and more melt water being released during winter. The projections for the 2090s show a large reduction in Qm_{prop} during summer and autumn. Interestingly, for WaSiM-Anderson, changes in Qm_{prop} are relatively small during the winter months.

To investigate the potential impact of the changes in the melt regime on the occurrence of flood events, the days when streamflow exceeded the HF-2y threshold were plotted for each month (Fig. 14). Fewer high flow events are projected during summer and autumn for the 2090s, while the number of days exceeding the HF-2y threshold increases dramatically between June and October. Despite obvious differences in the monthly melt regimes between Anderson and Tindex (Fig. 13), the role of the snow model is relatively unimportant as the monthly distribution of flood events is very similar for both the reference and 2090s periods (Fig. 14). This strongly suggests that the projected increase in flood events during winter and spring is primarily driven by the projected increase in precipitation and a reduction in the solid fraction, rather than by changes in the melt regime or, more specifically, the monthly occurrence of melt events.

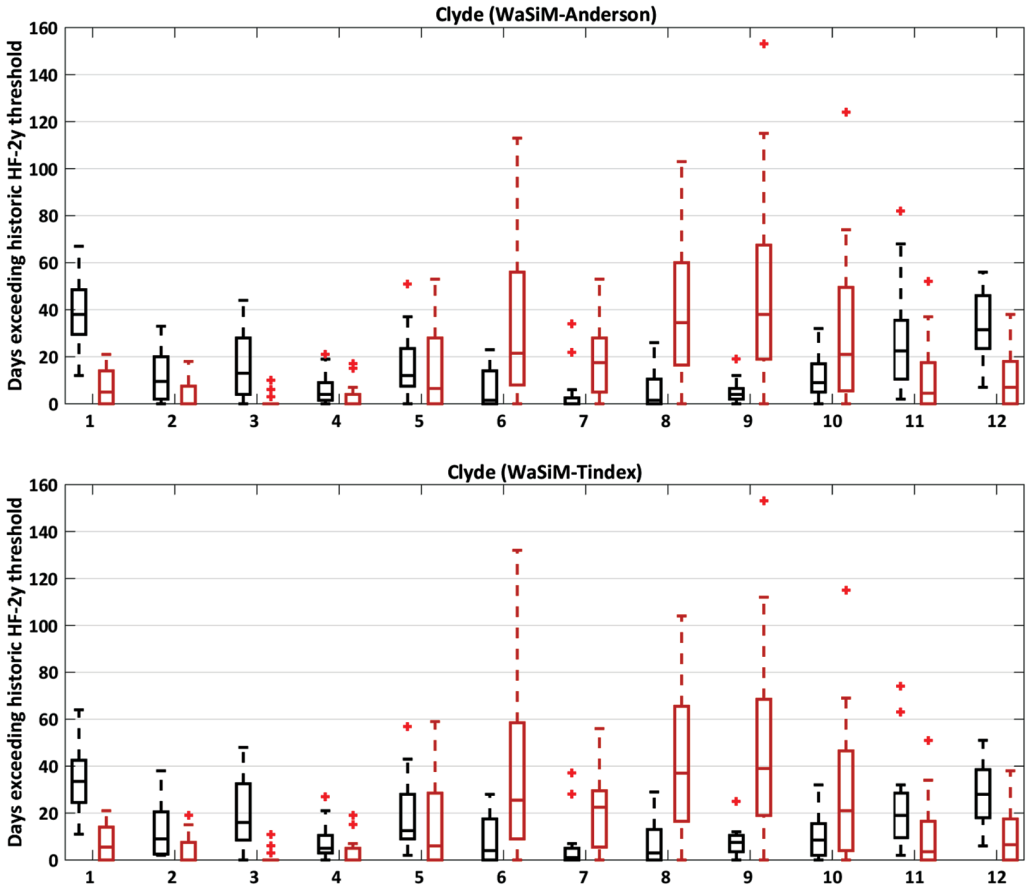

Figure 14 – The number of days (total number of days during the corresponding 19-year period) of streamflow exceeding a high flow event with a return period of two years (HF-2y) for each month. Black boxplots show the monthly values for the reference period and red boxplots for the 2090s. The HF-2y threshold is based on the reference period of the individual simulations.

Discussion

In this study, projected (2090s) increases in annual streamflow for both the A1B (12.5%) and A2 (10.7%) emission scenarios did not result in an equivalent increase in hydroelectric power output. These findings contrast with the much closer connection between river flow and hydroelectric power output shown in a number of previous studies from different alpine locations (e.g., Lehner *et al.*, 2005; Koch *et al.*, 2011; Chernet *et al.*, 2013). This apparent contradiction was most likely caused by an increasing number of days with the discharge exceeding the capacity of the scheme at Clyde, resulting in an increase in water being spilled. In the Waitaki catchment to the north of the Clutha, the projections of Caruso *et al.* (2016) also showed that the volume of spills will likely increase, and this was found to be predominantly caused by a substantial surplus of lake inflows during winter and spring. A potential explanation for the opposing finding reported by Chernet *et al.* (2013) could be the different water management schemes. The study of Chernet *et al.* (2013) was based on a relatively small

catchment (804 km^2) that is characterised by a high degree of water management (twelve regulated reservoirs and transfer tunnels), while the Clutha catchment only possesses one reservoir (Lake Hawea). Hence, it could be speculated that changes in seasonal streamflow and the frequency distribution of daily streamflow will have less impact in terms of changes to spill frequency in more intensively managed catchments.

For an alpine catchment in Switzerland, Finger *et al.* (2012) suggested that an increase in heavy precipitation events in the future would result in more high-water events causing an increased water loss due to overflow at schemes. The results of this study also suggest that an increase in heavy precipitation combined with a reduced snowfall-to-rainfall ratio are key drivers behind the projected increase in high flow events and related spills.

Regarding the driving mechanisms behind more frequent flood events, Arheimer *et al.* (2017) found these to be affected by both a decrease in snowfall and the duration of the snowpack. The results of this study suggest that the increase in flood events is primarily driven by changes in precipitation, more specifically: more winter precipitation, more extreme precipitation events and a reduced snowfall-to-rainfall ratio. For changes in heavy precipitation events, the positive trend was found to be strongest for the north-western headwaters of the catchment. This can likely be explained by the alpine location of the headwaters. In particular, the Dart River subcatchment extends further to the north-west towards the zone of peak Southern Alps precipitation described by Henderson and Thompson (1999), and also has a mean elevation greater than the other headwater subcatchments of the Clutha (indicative of a greater orographic uplift). Even with the relatively coarse (27 km) resolution of the RCM relative to the topographic complexity of the Southern Alps, orographic precipitation is still likely to have become more intense in the RCM simulations for the Dart River, causing the stronger trend in the extreme precipitation events.

In terms of potential impacts for the operators (i.e., Contact Energy), the increased output during winter and spring could be beneficial, while the decrease in output during summer could comprise periods when electricity demand is not met. Although any benefits may be tempered by seasonal price variations in the national electricity market, the potentially adverse effects during summer were also highlighted by Caruso *et al.* (2016) for the Waitaki, particularly if accompanied by an increased electricity demand (i.e., for cooling).

The decline in summer output could be mitigated by reducing the increased volume of spill water during winter and spring (due to the projected regime shift and an increase in flow events exceeding the capacity of Clyde) via new storages and adaptations in the water management of the Hawea outlet. Thus, the assumption that increased winter flow in the Southern Alps would reduce the need for reservoirs (Poyck *et al.*, 2011; Hendrikx *et al.*, 2012) is not supported by the findings of this study or the study of Caruso *et al.* (2016). Based on the projections of this study, increased artificial storage (i.e., dams, reservoirs) would be required to store some of the excess flow in winter and spring, which would then allow for the projected decreases in summer streamflow to be compensated, and ultimately sustain hydroelectric power output during summer. A similar finding came from the study of Hendrickx and Sauquet (2013), who investigated two catchments in the Pyrenees and found that early storage of winter runoff allows minimum flows during summer to be sustained.

It is the general consensus that, as for hydrological metrics (i.e., mean flow or SWE), studies targeting changes in hydroelectric power need to account for the uncertainty

introduced by the components of the model chain. While GCM, emission scenario and natural variability have been considered to be the main sources of uncertainty (Minville *et al.*, 2008), other components of the model chain might also be important (Wagner *et al.*, 2017). In the study of Finger *et al.* (2012) the main source of uncertainty varied depending on season (climate model for spring and autumn) and future period (hydrological parameters for summer and end of century). Here all simulations were consistent (except for some simulations in the 2050s) in terms of projecting an increase in output for winter and spring and a decrease for summer, albeit with a relatively large range (Fig. 6). Most of the spread could be attributed to the GCM and emission scenario (shown as combined effect in Fig. 6), where the bias correction and snow model have a comparably small effect. Thus, for the change in the seasonal output, bias correction and snow model (visibly stronger signal for WaSiM-Anderson compared to WaSiM-Tindex) also contribute to the overall uncertainty, but to a smaller extent.

The uncertainty analysis of the extreme flow indicators (HF and LF) identified the GCM and emission scenario as the primary sources of uncertainty, followed by bias correction and snow model. Thus, the large variability in the precipitation signal during winter and early spring is most likely the main mechanism affecting the range of HF and LF. Despite the role of the snow model being rather small, it is more important for LF, exceeding the contribution of the bias correction method for LF-2y and LF-5y.

Conclusion

The key findings for the Clutha encompass substantial seasonal changes in the hydroelectric power output due to projected changes in the seasonal streamflow regime under late 21st century climate change. Output based on the ensemble mean is projected to increase for winter (18%) and spring (7%), while changes for summer (-19%) and autumn (-4%) are negative. Further, an increase in spills is projected at the hydroelectric scheme, caused by a shift in the frequency distribution of daily streamflow towards events that exceed the maximum capacity of the scheme. Importantly, the results of this study indicate that the current water management in the Clutha catchment might be underdeveloped in terms of maximising hydroelectric generation under late 21st century climate conditions. Shortages could occur during summer, when reduced streamflow and more extreme periods of low flow could lead to a conflict of interest between irrigation and electricity demand.

The main driver behind the more frequent and extreme high flow events was found to be changes in precipitation, encompassing more winter precipitation, a reduction in the solid fraction of precipitation and an increase in extreme precipitation events. Emanating from the hydroclimate of the Clutha catchment, changes in the accumulation of snow are likely the main cause (as opposed to changes linked to the melt process) behind the rise in high flow events and linked spills. On a wider note, the modelling results from this study indicate that the implications of climate change for hydroelectric schemes in alpine environments can surpass the obvious changes in the annual or seasonal output. Thus, changes in the frequency of daily streamflow with more extreme high and low flow events could constitute a major challenge for run-off river schemes and current water management, even if seasonal changes towards a flatter regime suggest a reduced need for artificial storage. This study also demonstrated that inferring from an increase in annual streamflow to a corresponding increase in output might be misleading (again, due to more spills).

Regarding the uncertainty associated with the projections for hydroelectric output, most of the large variability was found to be caused by the GCM and emission scenario (with changes in seasonal precipitation as a key driver). The effects of bias correction and snowmelt method were smaller, but still added to the overall uncertainty of the ensemble.

Future work should examine whether our findings hold using the latest generation of climate model projections that are now available for the New Zealand domain (e.g., Eyring *et al.*, 2016) and explore the role of natural variability in the context of overall ensemble uncertainty. Different water management scenarios should also be investigated to see if the current infrastructure (i.e., the Hawea reservoir) would be able to reduce pressure during low flow periods in summer and reduce spills in winter and spring. In the event of increased spills (in both magnitude and frequency), assessment of the continued suitability of spillway capacity under changed hydroclimatic conditions may also become necessary.

Acknowledgements

We would like to thank a number of authorities who provided the various data sets used in this study. The National Institute of Water and Atmospheric Research (NIWA) for climate observations and the RCM simulations (particularly Abha Sood). Streamflow records were kindly provided by NIWA, Contact Energy Ltd. and the Otago Regional Council. The digital elevation model, soil data and land use information were obtained from Landcare Research New Zealand. This study was developed from work funded by a University of Otago Doctoral Scholarship to AMJ.

References

Arheimer, B.; Donnelly, C.; Lindström, G. 2017: Regulation of snow-fed rivers affects flow regimes more than climate change. *Nature Communications 8*: 62. https://doi.org/10.1038/s41467-017-00092-8

Beniston, M.; Stoffel, M. 2014: Assessing the impacts of climatic change on mountain water resources. *Science of the Total Environment 493*: 1129–1137. https://doi.org/10.1016/j.scitotenv.2013.11.122

Caruso, B.S.; King, R.; Newton, S.; Zammit, C. 2016: Simulation of climate change effects on hydropower operations in mountain headwater lakes, New Zealand. *River Research and Applications 33*: 147–161. https://doi.org/10.1002/rra.3056

Caruso, B.S.; Newton, S.; King, R.; Zammit, C. 2017: Modelling climate change impacts on hydropower lake inflows and braided rivers in a mountain basin. *Hydrological Sciences Journal 62(6)*: 928–946. https://doi.org/10.1080/02626667.2016.1267860

Chernet, H.H.; Alfredsen, K.; Killingtveit, Å. 2013: The impacts of climate change on a Norwegian high-head hydropower system. *Journal of Water and Climate Change 4(1)*: 17–37. https://doi.org/10.2166/wcc.2013.042

Chinn, T.J. 2001: Distribution of the glacial water resources of New Zealand. *Journal of Hydrology (New Zealand) 40(2)*: 139–187.

Collins, M.; Knutti, R.; Arblaster, J.; Dufresne, J.L.; Fichefet, T.; Friedlingstein, P.; Gao, X.; Gutowski, W.J.; Johns, T.; Krinner, G.; Shongwe, M.; Tebaldi, C.; Weaver, A.J.; Wehner, M. 2013: Long-term climate change: Projections, commitments and irreversibility. In: Stocker, T.F.; Qin, D.; Plattner, G.-K.; Tignor, M.; Allen, S.K.; Boschung, J.; Nauels, A.; Xia, Y.; Bex, V.; Midgley, P.M. (Eds.) *Climate Change 2013: The Physical Science Basis. Contribution of Working Group I to the Fifth Assessment Report of the Intergovernmental Panel on Climate Change*. Cambridge University Press, Cambridge, United Kingdom and New York, USA.

Cullen, N.J.; Conway, J. 2015: A 22 month record of surface meteorology and energy balance from the ablation zone of Brewster Glacier, New Zealand. *Journal of Glaciology 61(229)*: 931–946. https://doi.org/10.3189/2015JoG15J004

Cullen, N.J.; Gibson, P.B.; Mölg, T.; Conway, J.P.; Sirguey, P.; Kingston, D.G. 2019: The influence of weather systems in controlling mass balance in the Southern Alps of New Zealand. *Journal of Geophysical Research: Atmospheres 124*: 4514–4529. https://doi.org/10.1029/2018JD030052

Eyring, V.; Bony, S.; Meehl, G.A.; Senior, C.A.; Stevens, B.; Stouffer, R.J.; Taylor, K.E. 2016: Overview of the Coupled Model Inter-comparison Project Phase 6 (CMIP6) experimental design and organization. *Geoscientific Model Development 9(5)*: 1937–1958. https://doi.org/10.5194/gmd-9-1937-2016

Finger, D.; Heinrich, G.; Gobiet, A.; Bauder, A. 2012: Projections of future water resources and their uncertainty in a glacierized catchment in the Swiss Alps and the subsequent effects on hydropower production during the 21st century. Water Resources Research 48, W02521. https://doi.org/10.1029/2011WR010733

Gawith, D.; Kingston, D.G.; McMillan, H. 2012: The effects of climate change on runoff in the Lindis and Matukituki catchments, Otago, New Zealand. Journal of Hydrology (New Zealand) 51(2): 121–135.

Golombek, R.; Kittelsen, S.A.C.; Haddeland, I. 2012: Climate change: impacts on electricity markets in Western Europe. Climatic Change 113(2): 357–370. https://doi.org/10.1007/s10584-011-0348-6

Haguma, D.; Leconte, R.; Côté, P.; Krau, S.; Brissette, F. 2014: Optimal Hydropower Generation Under Climate Change Conditions for a Northern Water Resources System. Water Resources Management 28: 4631–4644. https://doi.org/10.1007/s11269-014-0763-3

Hamlet, A.F.; Lee, S.Y.; Mickelson, K.E.B.; Elsner, M.M. 2010: Effects of projected climate change on energy supply and demand in the Pacific Northwest and Washington State. Climatic Change 102: 103–128. https://doi.org/10.1007/s10584-010-9857-y

Henderson, R.D.; Thompson, S.M. 1999: Extreme rainfalls in the Southern Alps of New Zealand. *Journal of Hydrology (New Zealand) 38*: 309–330.

Hendrickx, F.; Sauquet, E. 2013: Impact of warming climate on water management for the Ariège River basin (France). *Hydrological Sciences Journal 58(5)*: 976–993. https://doi.org/10.1080/02626667.2013.788790

Hendrikx, J.; Hreinsson, E.Ö.; Clark, M.P.; Mullan, A.B. 2012: The potential impact of climate change on seasonal snow in New Zealand: Part I—an analysis using 12 GCMs. *Theoretical and Applied Climatology 110(4)*: 607–618. https://doi.org/10.1007/s00704-012-0711-1

Jiang, Y.; Liu, C.; Huang, C.; Wu, X. 2010: Improved particle swarm algorithm for hydrological parameter optimization. *Applied Mathematics and Computation 217*: 3207–3215. https://doi.org/10.1016/j.amc.2010.08.053.

Jobst, A.M.; Kingston, D.G.; Cullen, N.J.; Sirguey, P. 2017: Combining thin-plate spline interpolation with a lapse rate model to produce daily air temperature estimates in a data-sparse alpine catchment. *International Journal of Climatology 37(1)*: 214–229.

Jobst, A.M.; Kingston, D.G.; Cullen, N.J. 2018a: High resolution precipitation fields for the Clutha catchment. *Weather and Climate 38*: 2–14.

Jobst, A.M.; Kingston, D.G.; Cullen, N.J.; Schmid, J. 2018b: Intercomparison of different uncertainty sources in hydrological climate change projections for an alpine catchment (upper Clutha River, New Zealand). *Hydrology and Earth System Sciences 22*: 3125–3142. https://doi.org/10.5194/hess-22-3125-2018

Kerr, T. 2013: The contribution of snowmelt to the rivers of the South Island, New Zealand. *Journal of Hydrology (New Zealand) 52(2)*: 61–82.

Kienzle, S.W.; Schmidt, J. 2008: Hydrological impacts of irrigated agriculture in the Manuherikia catchment, Otago, New Zealand. *Journal of Hydrology (New Zealand) 47(2)*: 67–84.

Kingston, D.G.; Thompson, J.R.; Kite, G. 2011: Uncertainty in climate change projections of discharge for the Mekong River basin. *Hydrology and Earth System Sciences 15(5)*: 1459–1471. https://doi.org/10.5194/hess-15-1459-2011

Koch, F.; Prasch, M.; Bach, H.; Mauser, W.; Appel, F.; Weber, M. 2011: How will hydroelectric power generation develop under climate change scenarios? A case study in the Upper Danube basin. *Energies 4(12)*: 1508–1541. https://doi.org/10.3390/en4101508

Lehner, B.; Czisch, G.; Vassolo, S. 2005: The impact of global change on the hydropower potential of Europe: a model-based analysis. *Energy Policy 33(7)*: 839–855. https://doi.org/10.1016/j.enpol.2003.10.018

Lenderink, G.; Buishand, A.; Van Deursen, W. 2007: Estimates of future discharges of the river Rhine using two scenario methodologies: Direct versus delta approach. *Hydrology and Earth System Sciences 11(3)*: 1145–1159. https://doi.org/10.5194/hess-11-1145-2007

Leung, L.R.; Qian, Y.; Bian, X.; Washington, W.M.; Han, J.; Roads, J.O. 2004: Mid-century ensemble regional climate change scenarios for the Western United States. *Climatic Change 62(1-3)*: 75–113. https://doi.org/10.1023/B:CLIM.0000013692.50640.55

Liu, X.; Tang, Q.; Voisin, N.; Cui, H. 2016: Projected impacts of climate change on hydropower potential in China. *Hydrology and Earth System Sciences 20*: 3343–3359. https://doi.org/10.5194/hess-20-3343-2016

Madani, K.; Lund, J.R. 2010: Estimated impacts of climate warming on California's high-elevation hydropower. *Climatic Change 102(3-4)*: 521–538. https://doi.org/10.1007/s10584-009-9750-8

Majone, B.; Villa, F.; Deidda, R.; Bellin, A. 2016: Impact of climate change and water use policies on hydropower potential in the south-eastern Alpine region. *Science of The Total Environment 543*: 965–980. https://doi.org/10.1016/j.scitotenv.2015.05.009

Markoff, M.S.; Cullen, A.C. 2008: Impact of climate change on Pacific Northwest hydropower. *Climatic Change 87(3-4)*: 451–469. https://doi.org/10.1007/s10584-007-9306-8

Ministry of Economic Development 2012: *New Zealand Energy Data File. 2011 Calendar year edition*. Energy Information and Modelling Group, Ministry of Economic Development, Wellington, New Zealand.

Minville, M.; Brissette, F.; Leconte, R. 2008: Uncertainty of the impact of climate change on the hydrology of a nordic watershed. *Journal of Hydrology 358*: 70–83. https://doi.org/10.1016/j.jhydrol.2008.05.033

Mpelasoka, F.S.; Chiew, F.H.S. 2009: Influence of rainfall scenario construction methods on runoff projections. *Journal of Hydrometeorology 10(5)*: 1168–83. https://doi.org/10.1175/2009JHM1045.1

Muerth, M.J.; St-Denis, G.B.; Ludwig, R.; Caya, D. 2012: Evaluation of different sources of uncertainty in climate change impact research using a hydro-climatic model ensemble. In: Seppelt, R.; Voinov, AA.; Lange, S.; Bankamp, D. (Eds.) *2012 International Congress on Environmental Modelling and Software: Managing Resources of a Limited Planet*. International Environmental Modelling and Software Society Sixth Biennial Meeting, Leipzig, Germany.

Otago Regional Council 2008: *Surface water resources of Otago*. Dunedin, New Zealand.

Popescu, I.; Brandimarte, L.; Peviani, M. 2014: Effects of climate change over energy production in La Plata Basin. *International Journal of River Basin Management 12: 319–327*. https://doi.org/10.1080/15715124.2014.917317

Poyck, S.; Hendrikx, J.; McMillan, H.; Hreinsson, E.Ö.; Woods, R. 2011: Combined snow and streamflow modelling to estimate impacts of climate change on water resources in the Clutha River, New Zealand. *Journal of Hydrology (New Zealand) 50(2)*: 293–311. http://www.jstor.org/stable/43945028

Schulla, J. 2012: *Model description WaSiM*. Technical report, 324 pp. Available at http://wasim.ch

Shrestha, R.R.; Schnorbus, M.A.; Werner, A.T.; Berland, A.J. 2012: Modelling spatial and temporal variability of hydrologic impacts of climate change in the Fraser River basin, British Columbia, Canada. *Hydrological Processes 26*: 1841–1861. https://doi.org/10.1002/hyp.9283

Singh, P.; Bengtsson, L. 2004: Hydrological sensitivity of a large Himalayan basin to climate change. *Hydrological Processes 18*: 2363–2385. https://doi.org/10.1002/hyp.1468

Tait, A.; Henderson, R.; Turner, R.; Zheng, X. 2006: Thin plate smoothing spline interpolation of daily rainfall for New Zealand using a climatological rainfall surface. *International Journal of Climatology 26*: 2097–2115.

Wagner, T.; Themeßl, M.; Schueppel, A.; Gobiet, A.; Stigler, H.; Birk, S. 2017: Impacts of climate change on stream flow and hydro power generation in the Alpine region. *Environmental Earth Sciences 76*: 1–22. https://doi.org/10.1007/s12665-016-6318-6

Manuscript received 2 June 2020; accepted for publication 10 November 2021